Design and Simulation of Two Continues Wave AlGaAs/GaAs Semiconductor Cascade Quantum Well Lasers at Room Temperature

Banafshe Yaghtin[1], Rahim Ghayour[2] and Mohammad Hossein Sheikhi[3]
[1,2,3]Department of Electronic and Communication Engineering, Shiraz University, Iran
[1]b.yaqtin@yahoo.com

Abstract– **The objective of this research is to design and simulate two new structures of semiconductor quantum well cascade lasers. These structures are constructed of three quantum wells within their active regions, based on AlGaAs/GaAs materials. These structures are simulated in continuous wave (cw) mode and at room temperature. The first structure is a conventional type of cascade quantum well lasers and its output emitted power is 150 mW at the emission wavelength of 9.5 µm. In the second structure, the output power increased from 150 mW of the first structure to 210 mW at the same emission wavelength of 9.5 µm by three ways as follows: i) modifying the thicknesses of quantum wells and barriers, ii) varying mole fraction throughout the active regions, iii) reshaping the wells and conduction band in the active regions. The width, ridge cavity length and period numbers of both these lasers are 25um, 4 mm and 24 respectively. These two structures have a similar waveguide and cladding layers.**

Keywords– **Semiconductor Lasers, Quantum Wells and Quantum Cascade Lasers**

I. INTRODUCTION

Quantum cascade lasers (QCLs) are semiconductor quantum well lasers that based on intersubband transitions and carrier tunneling through the thin layers of nanometer thicknesses. Light amplification in these lasers by intersubband emission proposed by Suris and Kasarinove in 1971.

Then, after several years cascade quantum well lasers known by Jermo Faist in 1994 for first time. The first cascade quantum well laser fabricated based on InGaAs and InP materials. Thereafter, for first time in 1998 these lasers fabricated based on GaAs and AlGaAs. This invention developed the cascade quantum well laser performance in a vast range [1]. Semiconductor cascade quantum well lasers are consisted of several periods of quantum well and barrier layers of nanometer thicknesses [2]. In each period, some layers are as the active region and light emission occurs in this region. Each active layer can be consisted of one or several quantum wells. The other layers, which are between active regions, inject carriers into the active regions, where these layers called injector regions [3]. In these lasers, the emission wavelength depends on the thickness of quantum wells and barriers. Accordingly, this class of lasers can cover a broad range of emission wavelengths for different applications, where this is the most significant feature of these lasers. Quantum cascade lasers can emit wavelengths between 2.75 um to 250 um in both continuous wave mode and pulse mode at different temperatures [4].

Quantum cascade lasers with emission wavelength 3.8 to 9.5, have the best performance in continues wave mode and at room temperature.

These are accessible and significant lasers at present time [5]. Because of their vast range of emission wavelengths these lasers have different applications in military, medical, industrial, medical imaging, space optical communications and trace gas sensing fields [3], [4], [5]. In this research, we designed and simulated two quantum cascade lasers with enough large optical power at wavelength of 9.5 um in continuous wave mode and at room temperature.

II. EXPERIMENTS

A) Design of a Conventional GaAs QCL Structure and its Simulation Results

In this research, we have designed two GaAs injector based quantum cascade lasers that have a very simple structure with compare to most injector based lasers. These structures have only one GaAs well and two AlGaAs barriers as their injector regions and three GaAs quantum wells in there active regions. We elaborated the thickness of wells and barriers to have an emission wavelength of 9.5 µm and a large enough power. We designed the first structure based on $Al_{0.33}Ga_{0.67}As$/GaAs. Fig. 1 shows the whole structure of this laser. According to this figure, it has 24 period of active and injector regions that has sandwiched between two GaAs waveguides and cladding layers of 1um and 3.75um thicknesses respectively. This structure has a 25 um width and 4 mm ridge cavity length.

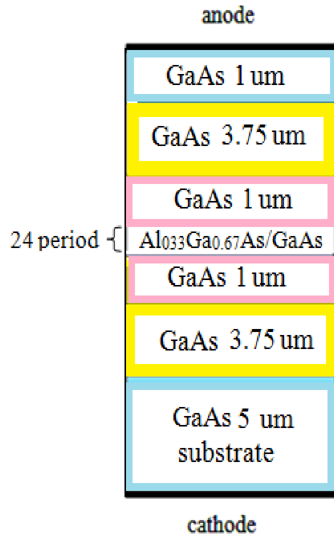

Fig. 1: Total structure of conventional Al0.33Ga0.67As/ GaAs QC laser

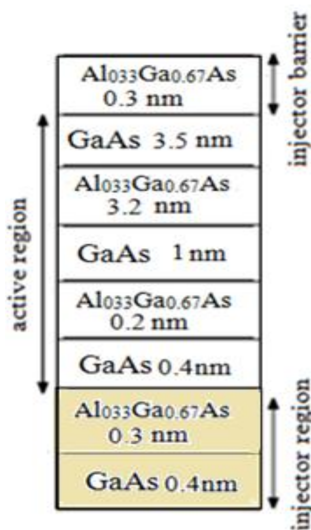

Fig. 2: The structure of active and injector regions per in one period of conventional $Al_{0.33}Ga_{0.67}As$/GaAs laser

Waveguide and cladding layers are Si highly doped to $n=19\times10^{19}cm^{-1}$ and $n=18\times10^{18}$ cm^{-1} respectively. This laser has a GaAs substrate layer with 5 um thickness which is highly Si doped to $n=19\times10^{19}cm^{-1}$. This layer is connected to cathode.

The thickness of top GaAs layer which is contacted to anode layer and is highly Si doped to $n=19\times10^{19}cm^{-1}$, is 1 um. The thickness of nanometer quantum well and barrier layers within one period are shown in Fig. 2, where it has only 8 layers. The colored layers of injector region in Fig. 2 are doped to $n=2\times10^{11}$ cm^{-1}. By solving Schrödinger equation in quantum wells, we have adjusted subbands for emission wavelength of 9.5 µm. Fig. 3 shows the conduction band and subband energies in the first period of this laser. An electric field 80 kv/cm is applied to make the first radioactive transition between two wells of the active regions in this structure.

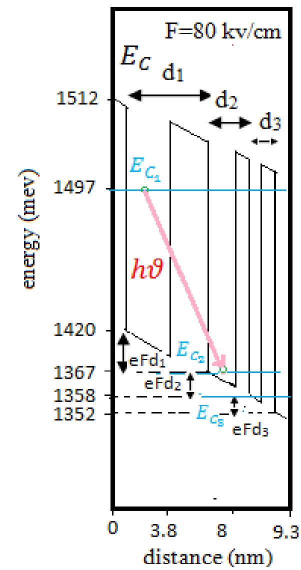

Fig. 3: Conduction band diagram for first period of $Al_{0.33}Ga_{0.67}As$/GaAs QC laser, the layer thicknesses in nm is beginning with $Al_{0.33}Ga_{0.67}As$ injector barrier from left to right are 0.3, **3.5**, 3.2, **1**, 0.2, **0.4**, 0.3, **0.4.** The numbers in bolds correspond to GaAs wells and normal numbers correspond to $Al_{0.33}Ga_{0.67}As$. The underlined numbers doped Si doped to $n=2\times10^{11}$ cm^{-1}

As Fig. 3 shows, the difference between subbands E_{C1}=1497 mev and E_{C2}=1367 mev, (ΔEc) is about 130 mev. When electrons stimulated to E_{C1} and population inversion occurs in this subband, a motive photon with about 130 mev energy, releases those electrons which populated in this subband. Thus, by tunneling through the barrier with thickness of 3.2 nm, electrons drop to E_{C2} and photon emission will occur. According to relation (1) in ref [7] the output optical wavelength of this laser will be about 9.5 um. In this relation h is planck's constant, c is light rate and E_{photon} is a motive photon energy.

$$\lambda = \frac{hc}{(E_{C_1} - E_{C_2})} = \left(\frac{hc}{E_{photon}} \right) \quad (1)$$

Then electrons tunnel through the barrier with thickness of 0.2 nm to go to E_{C3}. The lifetime of electrons that transport between E_{C2} and E_{C3} is less than the lifetime of electrons that transport between E_{C1} and E_{C2}. Therefore, electron transporting between E_{C1} and E_{C2} leads to phonon emission. By tunneling through the injector barrier with thickness of 0.3 nm, electrons can go to the injector region and relax to reach the next period. In the next period, the same action as that of the previous period happens and photon emission occurs. We have simulated this structure in continuous wave mode and at 300 K.

Fig. 4, shows this laser has a photon density of 1.8×10^{10} cm^{-1} at 9.5 um wavelength. As you can see in Fig. 5, this laser has a maximum output power of about 146 mw. The Current-Voltage characteristic at 300 K is shown in Fig. 6. Thereafter to increase the output power in wavelength of 9.5 um, we improved this structure by using of three different materials and reshaping wells in active regions. The improved structure introduced in next section.

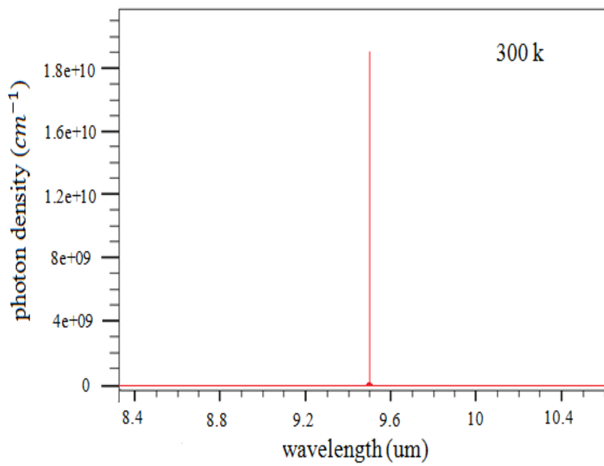

Fig. 4: The Photon Density-Wavelength characteristic of $Al_{0.33}Ga_{0.67}As$ QC laser in continuous wave mode and at 300k

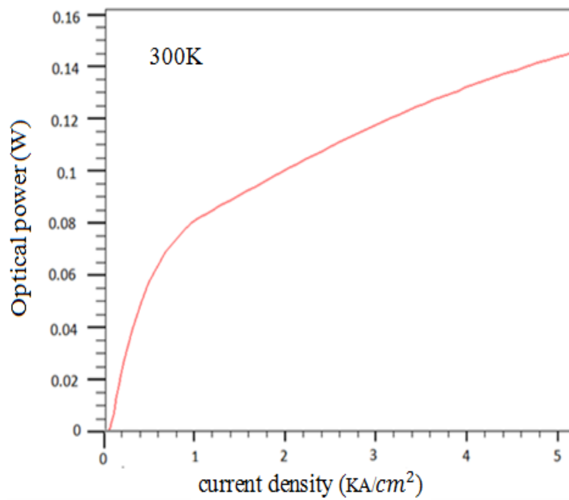

Fig. 5: The Output optical power-Current density characteristic of $Al_{0.33}Ga_{0.67}As$ QC laser in continuous wave mode and at 300k

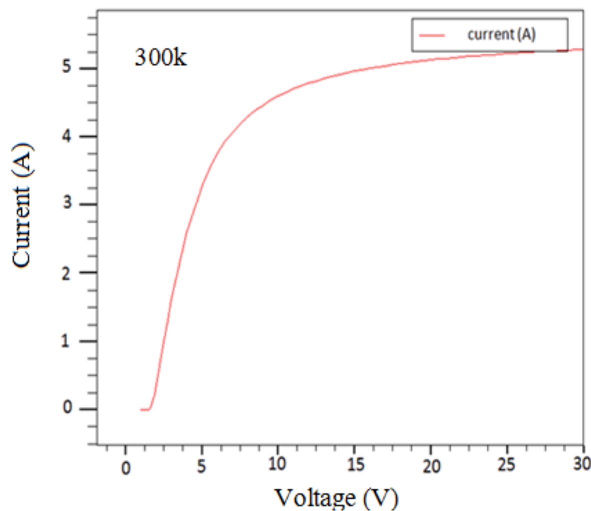

Fig. 6: The Current –Voltage characteristic of $Al_{0.33}Ga_{0.67}As$ QC laser in continuous wave mode and at 300k

III. DESIGN AND SIMULATION OF IMPROVED STRUCTURE

The second QC laser structure consists of $Al_{0.45}Ga_{0.55}As$ barriers, GaAs and $Al_{0.21}Ga_{0.79}As$ wells. This structure has 24 periods of active and injector regions that sandwiched between waveguide and cladding layers. The whole structure of this laser is similar to the previous structure and is shown in Fig. 7. However the thickness of quantum wells and barriers in each period are different as shown in Fig. 8.

As you can see in this figure, this structure has only 7 layers per each period. The layer thicknesses are adjusted to emit an optical wavelength of 9.5 um. The colored layers of injector regions in Fig. 8 are Si doped to $n=2\times10^{11}$ cm^{-1}. The conduction band of the first period and subband energies in quantum wells are shown in Fig. 9. As you can see in this figure, conduction band in active region have reshaped because of we used an $Al_{0.21}Ga_{0.79}As$ well in active region which has a more energy level than GaAs.

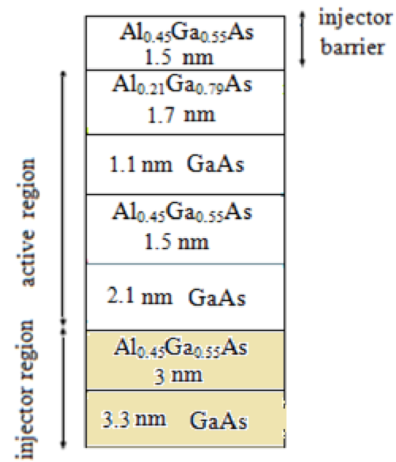

Fig. 7. Total improved QC laser structure

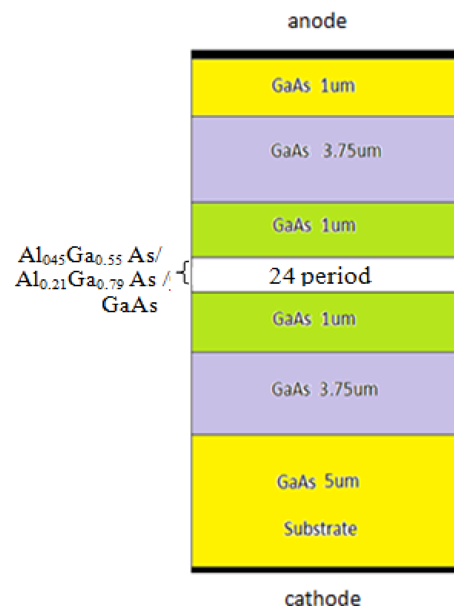

Fig. 8: One period of active and injector regions in improved structure

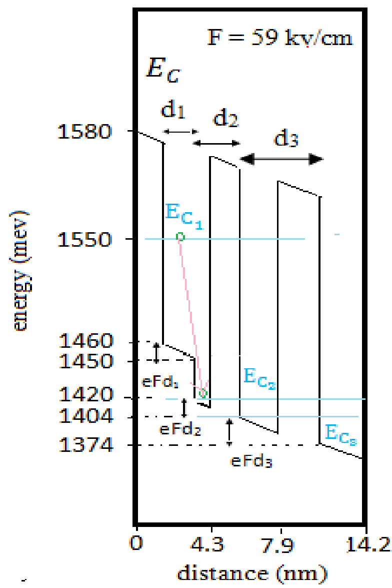

Fig. 9: Conduction band energy diagram at the first period of $Al_{0.21}Ga_{0.79}As$/ $Al_{0.45}Ga_{0.55}As$/ GaAs QC laser, the layer thicknesses in nm is beginning with $Al_{0.45}Ga_{0.55}As$ barrier, from left to right are: 1.5, *1.7*, **1.1**, 1.5, **2.1**, 3, **3.3**. The numbers in bolds correspond to GaAs well, normal numbers correspond to $Al_{0.45}Ga_{0.55}As$ barriers and bold italic number corresponds to $Al_{0.21}Ga_{0.79}As$ well. The underlined numbers are Si doped to $n=2\times10^{11}$ cm^{-1}

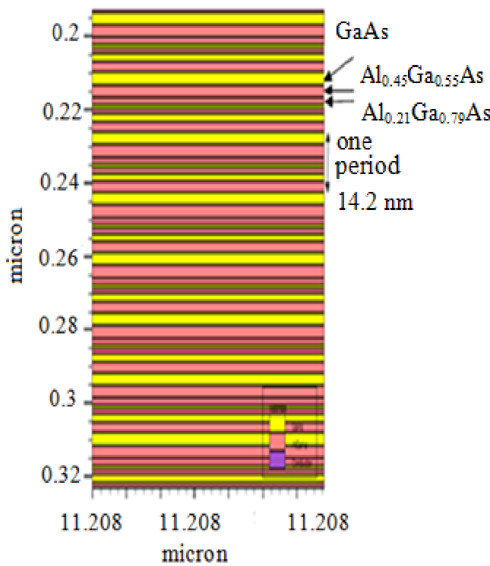

Fig. 10: A cross section of simulated active and injector nanometer layers in $Al_{0.21}Ga_{0.79}As$/ $Al_{0.45}Ga_{0.55}As$/ GaAs improved QC laser

IV. RESULTS AND DISCUSSION

According to Fig. 9 reshaping the conduction band of improved structure in section II leads to eliminate the barrier which is between E_{C1} and E_{C2} in the structure in section I. So, there is not any barrier in electrons direction from subband E_{C1} to E_{C2} subband in improved structure. Thus, electrons drop without any tunneling through their transport process from E_{C1} to E_{C2}. Tunneling electrons across the barriers causes interfaces between electrons and barrier lattice atoms. These interactions contribute to phonon emission and absorption losses. Thus, in this structure by eliminating the barrier between E_{C1} and E_{C2} losses decreased and as a result, lifetime of electrons (τ_{12}) will increase. According to equation (2) and (3), increase of (τ_{12}) leads to increase of effective lifetime of electrons (τ_{eff}) and differential gain (η_{tr}) [8].

$$\tau_{eff} = \tau_1(1 - \frac{\tau_2}{\tau_{12}}) \tag{2}$$

$$\eta_{tr} = \frac{\tau_{eff}}{\tau_{eff}+\tau_2} \tag{3}$$

Now, according to relation (4) increase of η_{tr} will result in increase of optical output power in this laser [9].

$$P = N_p \frac{\tau_{eff}}{\tau_{eff}+\tau_2} \frac{hw}{q_0} \frac{\alpha_m}{\alpha_m+\alpha_w} (J - J_{tr}) \tag{4}$$

In this relation N_p is the number of periods, hw is the motive photon energy, α_m is the mirror losses factor and α_w is the waveguide losses factor. Thus the second structure has a higher output optical power than structure in section I. We simulated improved structure in continues wave mode and at 300k. Some of simulated periods of this laser have shown in Fig. 10. As shown in Fig. 9, an electric field 59 kv/cm has been applied to this laser to emit the first photon. According to Fig. 9, photon emission occurs between E_{C1}=1550 and E_{C2} =1420 subbands. The energy difference between these two subbans, (ΔEc) is 130 mev. According to relation (1), by using motivation photon energy with 130 mev energy, this laser will emit an output optical wavelength of 9.5 um too. Fig. 10, shows this laser has a 2.4×10^{10} cm^{-1} photon density at 9.5 um wavelength. As Fig. 12 shows, this laser has a maximum output power of 210 mw at 300 k. I-V characteristic of this laser is shown in Fig. 13. Thus, in the wavelength of 9.5 um and at a lower electric field the improved structure has about 65 mw output optical power more than conventional one.

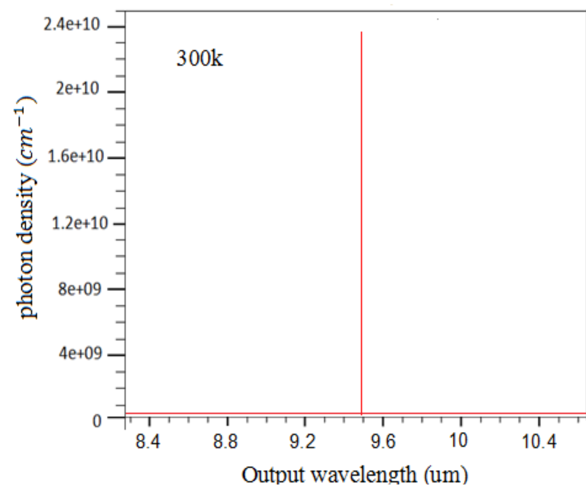

Fig. 11: Calculated output wavelength-photon density characteristic of $Al_{0.21}Ga_{0.79}As$/ GaAs $Al_{0.45}Ga_{0.55}As$ QC laser in continuous wave mode and at 300 k

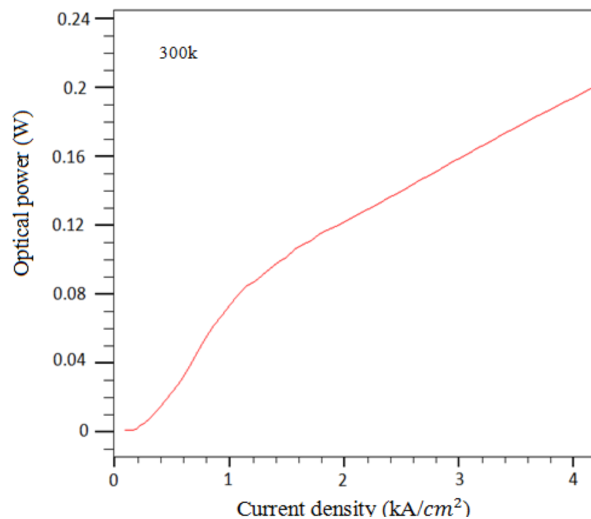

Fig. 12: Calculated output optical power-current density characteristic of $Al_{0.21}Ga_{0.79}As$/ GaAs/$Al_{0.45}Ga_{0.55}As$ QC laser in continuous wave mode and at 300 k

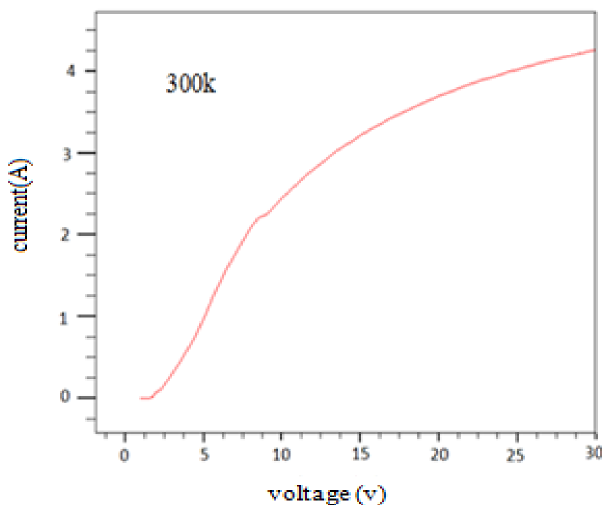

Fig. 13: Calculated current-voltage characteristic of $Al_{0.21}Ga_{0.79}As$/GaAs/$Al_{0.45}Ga_{0.55}As$ QC laser in continuous wave mode and at 300 k

V. CONCLUSION

In this work, by elaborating the layer thicknesses and subband energies, we designed two QC lasers. These structures designed for operating at room temperature and continues wave mode. The number of layers per each period is less with compare to most QC lasers. Therefore in these structures the electron interactions and scatterings decrease and it leads to reduce absorption losses and increase output power. In addition by using of three different mole fractions in active regions, we reshaped conduction band and we could eliminate the barrier which is between two wells in active regions of conventional structure. Therefore, in structure II the losses of electron transport and photon emission which are because of electron tunneling through this eliminated barrier will decrease and it leads to increase optical output power of structure II in a considerable value.

ACKNOWLEDGEMENT

The author would like to acknowledge Dr. Ghayour and Dr. Sheykhi from electronic and communication engineering department of Shiraz University for their supports and helpful guidance in this research.

REFERENCES

[1]. Faist Jermo, Cappasso Federico, Deborah L. Sivco, Carlo Sirtori, Albert L, *Quantum cascaded Laser,* Science 264, 553-556, (1994).

[2]. Wanga, C.A., Goyal, A.K., S.Menzel, Calawa, D.R., Connors, M.K., Sanchez, A., Turner, G.W., Capasso, F., Highpower, *λ~9.6 um tapered quantum cascade lasers grown by OMVPE*, Journal of Crystal Growth 370, 212–216, (2013).

[3]. Katz Simeon, Augustinas Vizbaras, Ralf Meyer and Markus Amann, *Injectorless quantum cascade lasers*, Journal of Appl.Phys.109, 081101, (2011).

[4]. Bekin, N.A., Pavlov, S.G., *Quantum cascade laser design based on impurity–band transitions of donors in Si/GeSi (111) heterostructures,* Physica B. 404, 4716, (2009).

[5]. Kamil Kosiel, JustynaKubacka-Traczyk, PiotrKarbownik, AnnaSzerling, *Molecular-beam epitaxy growth and characterization of mid-infrared quantum cascade laser structures, Microelectronics Journal* 40, 565– 569, (2009).

[6]. Xujiao Gao, Month carlo, *simiulation of Electron dynamics in quantum cascaded lasers*, A dissertation submitted in partial fulfillment of the requirements for the degree of Doctor of Philosophy, (Electrical Engineering) at the university of wisconsin–madison, 2008.

[7]. Jerome Faist, Federico Capasso, Deborah L. Sivco, Carlo Sirtori, Albert L. Hutchinson, Alfred Y. Cho, *Quantum Cascade Laser, Science*, Vol. 264, 1994.

[8]. Faist Jerom, Cappasso, Federico, *Intersubband Optoelectronics,* ETH Zurich, 2009.

[9]. Kale J. Franz, Matthew D. Escarra, Anthony J. Hoffman, Peter Q. Liu,1 James J.J. Raftery, Scott S. Howard, *Short Injector Regions for Improved Quantum Cascade Laser Performance*, Department of Electrical Engineering, Princeton University, 2008.